Fibers and Polymers 2009, Vol.10, No.5, 569-575 DOI 10.1007/s12221-010-0569-8

Synthesis and Characterization of Polyurethane-based Side-chain Cholesteric Liquid Crystal Polymers

R. N. Jana[1] and Jae Whan Cho*

Department of Textile Engineering, Konkuk University, Seoul 143-701, Korea
[1]Artificial Muscle Research Center, Konkuk University, Seoul 143-701, Korea
(Received March 28, 2009; Revised May 8, 2009; Accepted June 19, 2009)

Abstract: Polyurethane-based side-chain cholesteric liquid crystalline polymers (ChLCPs) with variable clearing temperatures were synthesized in a two-step reaction. The chemical structures of ChLCPs were confirmed by FT-IR and ^{1}H-NMR spectroscopy. The mesogenic properties and phase transition behavior were investigated by means of differential scanning calorimetry (DSC), polarizing optical microscopy (POM), and X-ray diffraction measurements. The DSC studies show that the melting temperature and isotropic transition temperature of the ChLCPs increased with the weight percentage of cholesterol in the polymer. POM shows that the ChLCPs had a distinct spherulite structure that melted at about 140 °C, and these results are consistent with those of the DSC studies. The thermogravimetric studies show that the ChLCPs were stable up to 200 °C, though there was a reduction in the thermal stability as the weight proportion of cholesterol and glycerol in the polymer increased.

Keywords: Side-chain cholesteric liquid crystalline polymer, Polyurethane, Mesogen, Thermal property

Introduction

Liquid crystal polymers (LCPs) have attracted considerable attention due to their potential application in numerous areas, such as gas detectors [1], nonlinear optics [2,3], temperature detectors [4], optical information storage devices [5,6], and piezoelectric generators [7]. There is a special type of LCP known as chiral nematic liquid crystal or cholesteric LCP (ChLCP): its molecules are gradually twisted against each other to form a helicoidal structure. As the length of the pitch corresponds to the wavelength of light, the light can be reflected from the polymer with different levels of efficiency. The coloration of the reflected radiation depends on the ambient temperature, and the length of the pitch increases as the temperature increases. Thus, ChLCPs can often be used for temperature detection [4].

For recent potential ChLCP applications in different fields, further systematic studies are needed on the different parameters, such as molecular structure and chirality, which influence the properties of ChLCPs. The LCP molecular structure, on which the liquid crystalline properties are largely dependent, can be divided into three main structural parts: a flexible polymer chain, a spacer, and a mesogenic unit. The spacer should have sufficient length and be flexible enough to absorb the motion coming from the polymer backbone in order to resist any disturbance to the crystalline zone of the mesogen [8]. Because of the complexity of the system, it is very difficult to determine the effect of individual variables on liquid crystalline behavior. However, several systematic investigations have endeavored to find the correlation between the above-mentioned variables and the liquid crystalline behavior [9-13]. Most of the research refers to LCPs with an acrylic [14], methacrylic [15], or siloxane backbone [16,17] and only a limited number of works refer to polyurethane-based LCPs [18-20].

In this study, we report on the synthesis of a series of ChLCPs; the synthesis involves a two-stage reaction of poly(ε-caprolactone)diol (PCL), 4,4'-methylene bis(phenyl isocyanate) (MDI), glycerol and cholesterol. Polyurethane composed of PCL, MDI, and glycerol was used as a main chain with PCL, MDI and glycerol, and mesogenic monomer cholesterol was formed as a side chain via MDI. We also discuss the effect of cholesterol on the mesogenic properties, thermal stability, and crystallization behavior.

Experimental

Materials

For this study, we used PCL (Mw=3000 g/mol) from the Solvay Co., U.K., MDI from Sigma Aldrich, USA, glycerol from Shinyo Pure Chemicals, Japan, and cholesterol from Aldrich-Sigma, USA.

Synthesis of LCPs

The LCPs were prepared in a two-step process (Figure 1). In the first step, a polyurethane block copolymer was synthesized from its monomers MDI, PCL, and glycerol in different mol ratios (of 4:3:1, 4:2:2 and 4:1:3) at 80 °C for 90 min in a four neck cylindrical vessel equipped with a mechanical stirrer under a nitrogen flow. In the PU, PCL acted as a soft segment, whereas MDI and glycerol acted as the hard segments. In the second step, approximately 100 m*l* of dimethylformamide (DMF) was added to the neat PU; the temperature was maintained at 80 °C; the required quantity of cholesterol with an equimolar proportion of MDI was added; and the reaction was continued for another 30 min.

*Corresponding author: jwcho@konkuk.ac.kr

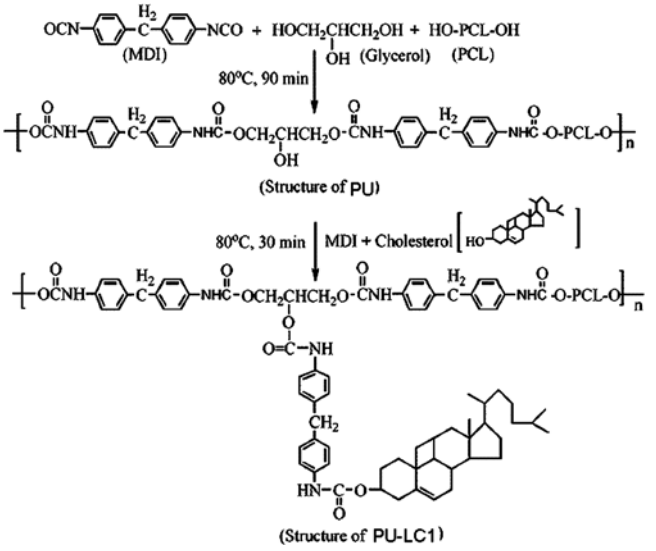

Figure 1. Schematic diagram for the preparation of LCPs.

Table 1. Compositions for PU and PU based LCPs

Sample code	MDI (mol)	PCL (mol)	Glycerol (mol)	Cholesterol (mol)	Cholesterol (mol %)
PU	4	3	1	0	0
PU-LC1	4+1*	3	1	1	10.0
PU-LC2	4+2*	2	2	2	16.7
PU-LC3	4+3*	1	3	3	21.4

Mol of MDI added in the 2nd stage reaction.

The samples were coded as PU, PU-LC1, PU-LC2 and so on, and the cholesterol proportion was varied from 0 to 21.4 mol% (Table 1). The yield in every case was about 95 %.

Characterization

Fourier transform infrared (FT-IR) spectroscopic measurements were performed with a Jasco FT-IR 300E device in accordance with an attenuated total reflectance method. For the ^{1}H-NMR characterizations, we used a Bruker Advanced DMX 500 spectrometer. The samples were prepared in $CDCl_3$ at room temperature.

Thermogravimetric (TG) and derivative thermogravimetric (DTG) analyses of the samples were carried out in a thermogravimetric analyzer (TGA Q500). The studies were done in a nitrogen atmosphere at a heating rate of 10 °C/min. Wide-angle X-ray scattering (WAXS) with monochromatized CuK_α radiation was carried out by using an X-ray diffractometer (Bruker AXS). The area ratio of crystalline peaks to the total area of crystalline and amorphous peaks was used as the measure of crystallinity. Differential scanning calorimetric (DSC) measurements were taken with a TA instrument 2010 thermal analyzer at a heating rate of 5 °C/min in nitrogen and a cooling rate of 2 °C/min.

To observe the visual textures and phase transition temperatures for analysis of the mesomorphic properties of the liquid crystalline polymers, we used a polarized optical microscope (Eclipse LV 100 POL) from the Nikon corporation, Tokyo, Japan, which was equipped with a hot stage (LTS 350) from Linkon Scientific Instruments Ltd., England, UK. The samples used for the polarizing optical microscopy (POM) analysis were sandwiched between two glass cover slips and melted on a hot stage at 200 °C, with care being taken to avoid cover slip sliding as that would lead to void formation; and the samples were subsequently cooled to room temperature. The temperature ramping rates were chosen to be consistent with the DSC.

Results and Discussion

Formation of a PU-based LCP as Confirmed by FT-IR and ^{1}H-NMR Studies

The FT-IR spectra for the PU and PU-LC1 are illustrated in Figure 2. The peak at 2925 cm^{-1} is due to stretching vibration of the C-H associated with the aromatic ring of the MDI. A weak peak at 2859 cm^{-1} is assigned to the C-H deformation of the aliphatic chain of glycerol and/or PCL [21]. We observed a peak at 1727 cm^{-1}, which corresponds to the carbonyl group of the urethane linkage; a sharp peak at 1662 cm^{-1} for the associated C-N, a peak at 1380 cm^{-1} for the C-H deformation of glycerol; and peaks at 1253 cm^{-1} and 1083 cm^{-1} for the C-O-C stretching of the backbone chain [21]. The subtracted spectrum (of PU-LC1 minus PU) in Figure 2 shows a peak at 1746 cm^{-1}; this peak, which corresponds to the urethane carbonyl, indicates an additional reaction of MDI with the remaining -OH of PU as shown in Figure 1. Another peak at 1370 cm^{-1}, which is for the C-H deformation of the aliphatic chain (-CH_2-) of cholesterol, confirms the expected attachment of cholesterol in the molecular structure of the LCP.

Figure 3 shows a ^{1}H-NMR spectrum of PU. The aliphatic protons of the glycerol in the O-CH_2-CH(OH)-CH_2-O appear

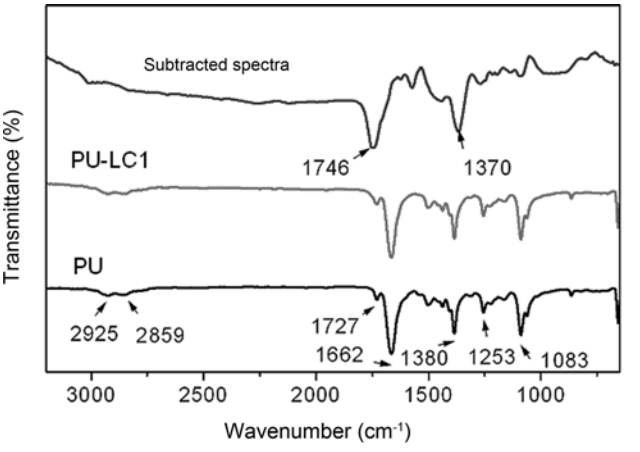

Figure 2. FT-IR spectra of PU, PU-LC1 and their subtracted spectra.

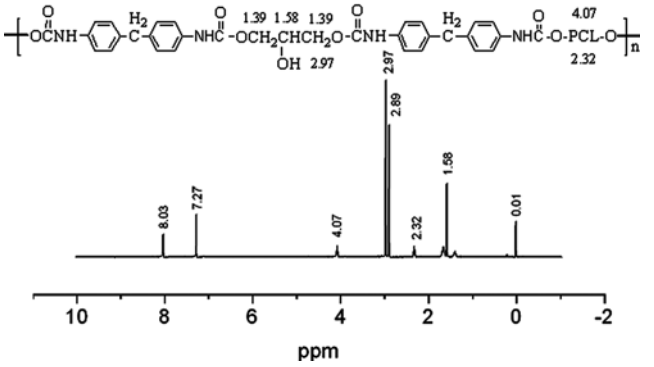

Figure 3. Chemical shifts for PU and their assignments.

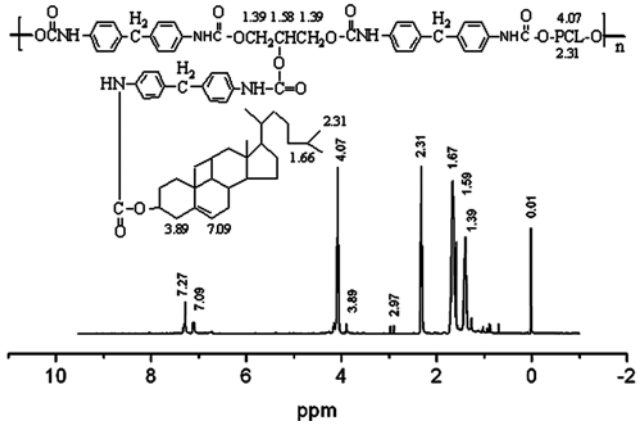

Figure 4. Chemical shifts for PU-LC1 and their assignments.

at 4.07 ppm, whereas the protons of O-CH_2-CH_2- from the PCL are observed at around 2.32 ppm to 2.97 ppm [21,22]. The presence of resonance peak at around 8.03 ppm is attributed to the aromatic protons from the MDI unit [21]. The results also confirm the formation of polyurethane from MDI, glycerol and PCL. As shown in the ^{1}H-NMR spectrum of PU-LC1 in Figure 4, besides all the other peaks for PU, some extra peaks formed as a result of the addition of cholesterol; for example there is a peak at 3.89 ppm for protons from the cyclic unsaturation of cholesterol, and peaks at around 1.66 to 2.31 for the aliphatic chain of cholesterol [23]. Thus, ^{1}H-NMR also confirms that cholesterol is added as a side chain to the backbone of polyurethane via an MDI molecule as described earlier (Figure 1).

Effect of Cholesterol on the Phase Transition Behavior

The liquid crystalline phase transition behavior of the LCPs was determined by DSC. As shown in Figure 5, the polymers reveal crystal melting (T_m) at about 51 °C to 52 °C and, except for the PU, all the other polymers show an isotropic transition temperature (T_i) at about 139 °C to 145 °C. The T_m of the PU only occurs at 50.6 °C with no T_i, because there is no mesogen unit in this composition (Table 1) and it is just a polyurethane elastomer. Note also that the

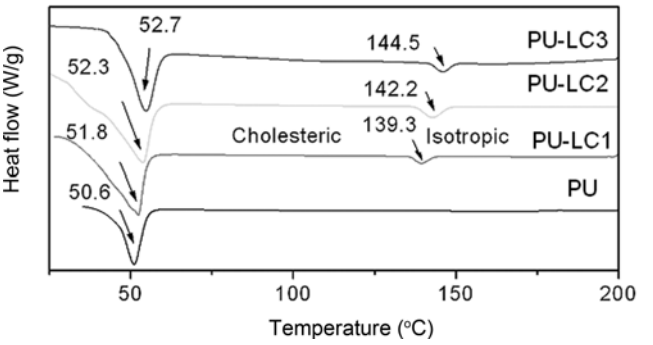

Figure 5. DSC traces for the LCPs.

T_m values of PU and PU-LC3 are shifted towards higher values. For SCLCPs, the T_m value tends to be influenced by the polymer backbone, the mesogenic group, the flexible spacer length, and the cross-linking density (C_x). The chemical crosslinking imposes additional constraints on the motion of chain segments, thereby causing an increase in the T_m value [24]. Thus, with the weight percentage of cholesterol increasing from 0 to 21.4 mol wt%, T_m increases from 50.6 °C for PU to 52.7 °C for PU-LC3. Again, with the increasing mol% of cholesterol, the T_i value increases from 139.3 °C for PU-LC1 to 144.5 °C for PU-LC3.

Effect of Cholesterol on the Thermal Stability

Figure 6 shows TG and DTG curves of the LCPs, and their corresponding degradation temperatures are presented in Table 2. When the weight percentage of cholesterol in the polymers increases, there is a decrease in the following: the initial degradation temperature (T_1) corresponding to a 1 % decomposition for the polymers; the maximum decomposition temperatures (T_{max}), where the DTG curves show a peak; the temperature at which 50 % of the materials has decomposed (T_{50}); and the temperature at the finish (T_f), where no more appreciable degradation is possible. For instance, the T_1 values for PU to PU-LC3 are 238 °C, 129 °C, 97 °C and 81

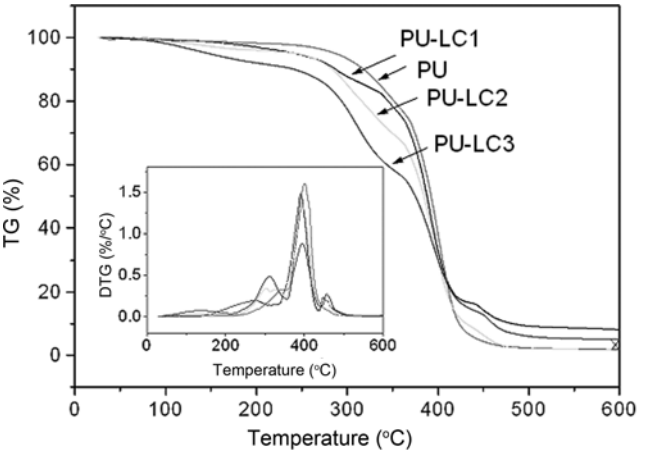

Figure 6. TG and DTG curves for the LCPs.

Table 2. Thermogravimetric analysis of PU and PU based LCPs

Sample	T_1 (°C)	T_{1max} (°C)	T_{2max} (°C)	T_{3max} (°C)	T_{50} (°C)	T_f (°C)
PU	238	339	400	-	392	510
PU-LC1	130	331	398	448	388	495
PU-LC2	98	326	395	446	384	491
PU-LC3	82	312	394	445	375	489

Note: T_1: Initial degradation temperature, T_{1max}: 1st maximum decomposition temperature, T_{2max}: 2nd maximum decomposition temperature, T_{3max}: 3rd maximum decomposition temperature, T_{50}: temperature at which 50 % of the material has been degraded, T_f: temperature of finish after which no appreciable degradation is possible.

°C, respectively. It is also clear from the thermograms that all other polymers except PU show three-stage degradation whereas PU shows two-stage degradation. The maximum decomposition temperatures (T_{1max}, T_{2max}, and T_{3max}), which are the temperatures at which the TGA curves show peak maxima, become the highest for PU (e.g., T_{1max}= 339 °C and T_{2max}=400 °C). Thus, PU is the most thermally stable polymer because it contains either a high proportion of PCL, which is a saturated backbone, or a rather low proportion of glycerol (Table 1), which is a secondary hydrogen-containing component that is more prone to thermal oxidation than the primary component (saturated backbone).

Another reason for the lower thermal stability of the polymers with a higher content of glycerol may be the higher density of crosslinks. As the weight proportion of glycerol in the polymer increases, the possibility of forming crosslinks also increases. If more crosslinks are formed, the network structure becomes more strained and the polymers consequently become more susceptible to thermal oxidation [25]. Therefore, the thermal stability of LCPs decreases with the increasing weight percentage of cholesterol in the polymers. Moreover, all the LCPs show a negligible weight loss up to 200 °C, which means they are sufficiently resistant to thermo-oxidative decomposition.

Effect of Cholesterol on the Degree of Crystallinity

WAXS measurement was performed on the samples to investigate the crystallization behavior of the polymers. With regard to PCL, the results show crystallization peaks near the WAXS region. The WAXS patterns for PCL and the synthesized polymers, which are depicted in Figure 7, show that PCL has diffraction peaks near 2θ= 21.44 ° and 23.81 ° for the (110) and (200) reflections, respectively [26]. Similar peaks can also be observed in the polymers when the peak intensity decreases; hence, the peaks in the polymers are likely due to the presence of PCL crystalline chain segments in the PU chain. From the XRD patterns, the degree of crystallinity (X_c) in the PCL is about 34.7 % while the corresponding values for the synthesized polymers, PU to PU-LC3, are 26.2 %, 14.8 %, 8.9 % and 5.3 %, respectively. This outcome indicates that the crystallinity of PU is lower than that of PCL because the bulky MDI in the PU chain, as well as the cholesterol (i.e., for PU-LC1 to PU-LC3) and the crosslinking, may impair the crystallization process of the PCL chain in the polymer. The residual low crystallinity for PU-LC1 to PU-LC3 may be due to the close packing of cholesterol via the crosslinking of glycerol [27,28].

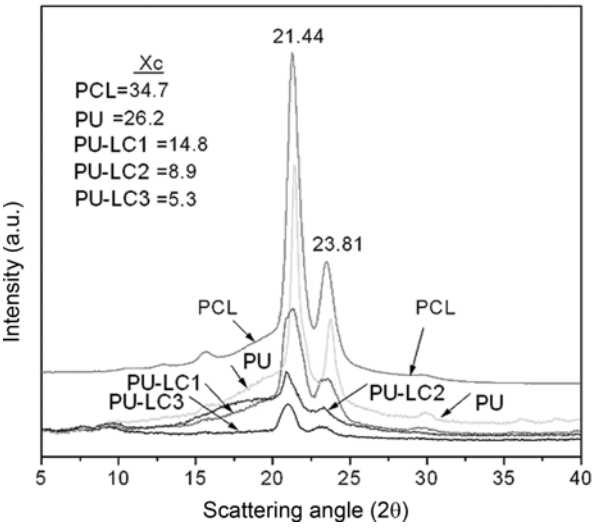

Figure 7. WAXS patterns for PCL and LCPs.

Polarized Optical Microscopy

The optical textures of PCL, cholesterol and polymers were characterized by POM with a hot stage. The POM photographs taken after the PCL had been cooled to room temperature exhibit a spherulite structure (Figure 8(a)) [29]. When the cholesterol was heated to 147 °C, the sample began to melt into a typical cholesteric oily texture, and a broken focal-conic texture appeared; however, the texture disappeared at 148 °C. When the isotropic state was cooled to room temperature, a bright focal-conic texture with selective color reflections from the different planes appeared [30], as shown in Figure 8(b). The PU did not show any sharp crystalline phase morphology under POM, though it had 26.2 % crystallinity as measured by WAXS. There are numerous color spots on the surface of the POM image, indicating that the nucleation for PCL crystallization has been started, though it will take a somewhat longer time to be completely grown (Figure 9(a)). In contrast, PU-LC1 and PU-LC2 show a spherulite structure (Figure 9(b) and 9(c))

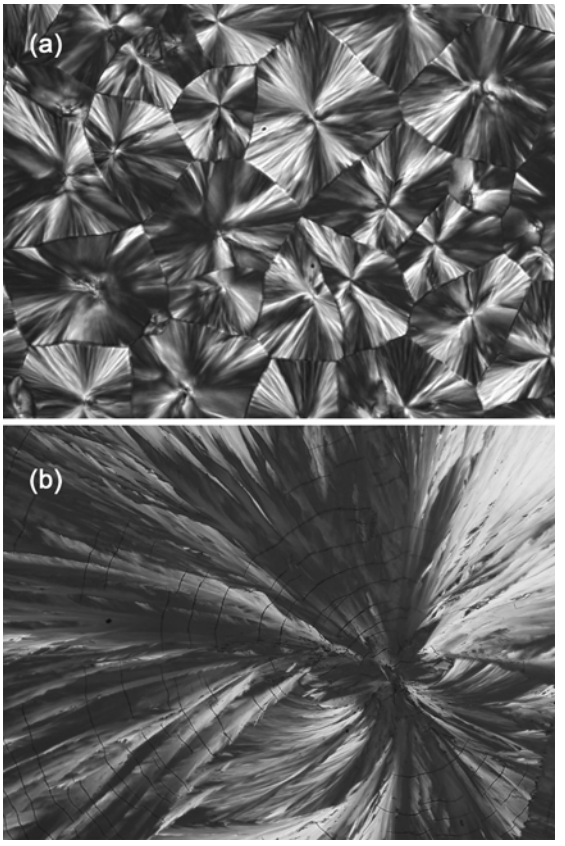

Figure 8. POM phase morphology at 20 °C of (a) PCL (500×) and (b) cholesterol (200×).

and PU-LC3 shows a hollow lake-like multidomain structural characteristic with the type of crystal structure expected from a highly crosslinked LC network (Figure 9(d)). A significant decrease in the transmittance was also observed for PU-LC3 (Figure 9(d)). The transformation from a uniaxial monodomain structure to a multidomain structure with the addition of a high percentage of the crosslinking agent of glycerol may be related to the shrinkage associated with the crosslinking; this transformation may also be one of the factors that lead to the disorder of the macroscopic molecular orientation [31]. Consequently, the multidomain structure is responsible for a significant decrease in the transmittance due to strong light scattering.

An image of the structural changes during the heating of the PU-LC1 sample is shown in Figure 10; it shows the POM of the polymer at a magnification of 100 at three different temperatures of 138 °C, 139 °C, and 140 °C. This image shows that there was no melting up to 138 °C: rather, the melting started at 139 °C and was completed at 140 °C. These results are consistent with the DSC results of the PU-LC1 polymer.

Conclusion

Polyurethane-based ChLCPs were synthesized successfully from PCL, MDI, glycerol and cholesterol in a two-step reaction. The mesogenic properties and phase transition behavior in the DSC studies show that the melting temperature and isotropic transition temperature of the ChLCPs increase

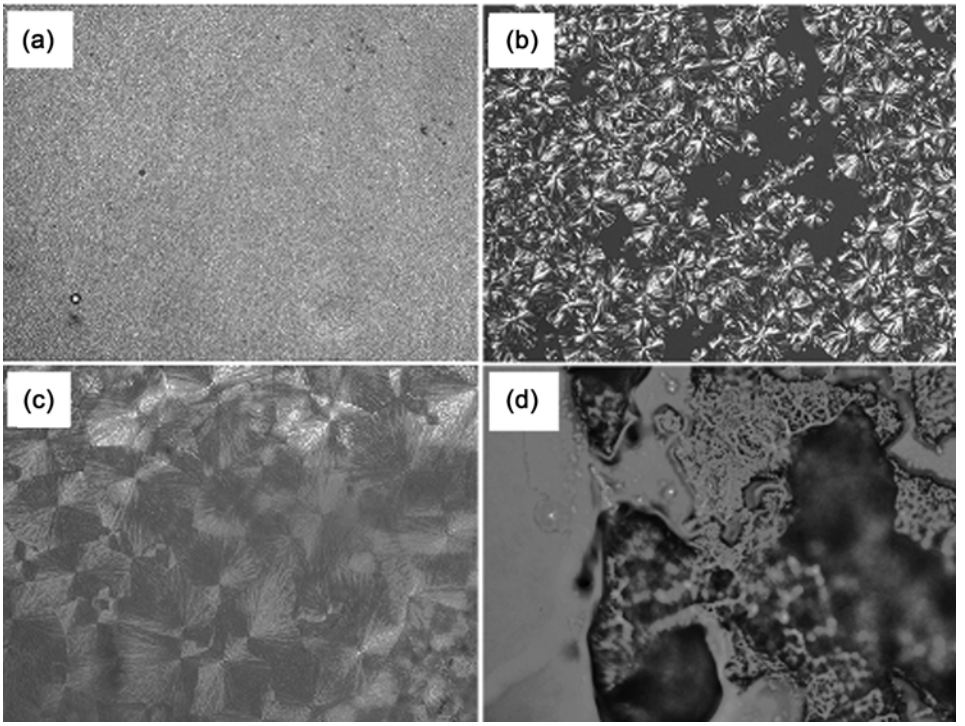

Figure 9. POM phase morphology (200×) at 20 °C for the different polymers (a) PU, (b) PU-LC1, (c) PU-LC2, and (d) PU-LC3.

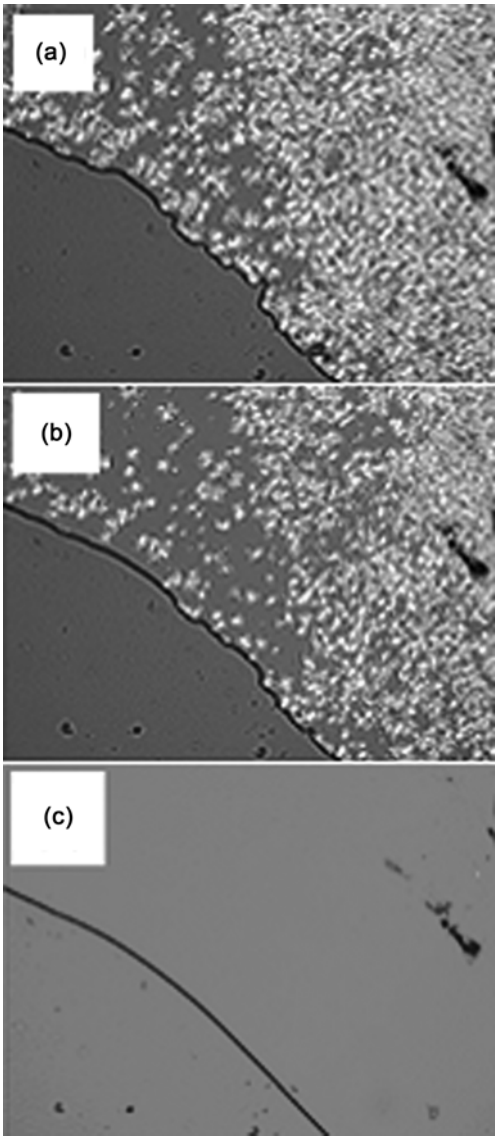

Figure 10. POM phase morphology (100×) for PU-LC1 at different temperatures (a) 138 °C, (b) 139 °C, and (c) 140 °C.

as the weight percentage of cholesterol in the polymers increases. POM shows that the PCL has a spherulite crystal structure whereas the cholesterol has a focal-conic structure. However, the ChLCPs with a low mol% of cholesterol have a spherulite crystal structure, whereas those with a high mol% of cholesterol have no crystal structure but a hollow lake-like multidomain structure. The TGA studies show that the thermal stability of the polymer decreases as the mol% of cholesterol in the polymers increases, though the synthesized ChLCPs are sufficiently stable up to 200 °C.

Acknowledgements

This work was supported by a grant from the Korea Research Foundation Grant (KRF-2006-005-J03302).

References

1. C. Carfagna, E. Amendola, G. Mensitieri, and L. Nicolais, *J. Mater. Sci. Lett.*, **9**, 1280 (1990).
2. M. Chen, L. Yu, L. R. Dalton, Y. Shi, and W. H. Steier, *Macromolecules*, **24**, 5421 (1991).
3. M. Trollsas, F. Sahlen, U. W. Gedde, A. Hult, D. Hermann, P. Rudquist, L. Komitov, S. T. Lagerwall, B. Stebler, J. Lindstrom, and O. Rydlund, *Macromolecules*, **29**, 2590 (1996).
4. N. Kirchner, L. Zedler, T. G. Mayerhofer, and G. J. Mohr, *Chem. Commun.*, **14**, 1512 (2006).
5. M. S. Ho, A. Natansohn, and P. Rochon, *Macromolecules*, **29**, 44 (1996).
6. X. Meng, A. Natansohn, C. Barrett, and P. Rochon, *Macromolecules*, **29**, 946 (1996).
7. C. C. Chang, L. C. Chien, and R. B. Meyer, *Phys. Rev. E*, **55**, 534 (1997).
8. V. Percec and C. Pugh in "Side Chain Liquid Crystal Polymers" (C. B. McArdle Ed.), Chap.3, Glasgow, Blackie, 1989.
9. A. A. Craig and C. T. Imrie, *Macromolecules*, **28**, 3617 (1995).
10. C. T. Imrie, F. E. Karasz, and G. S. Attard, *Macromolecules*, **26**, 3803 (1993).
11. V. Percec and A. Keller, *Macromolecules*, **23**, 4347 (1990).
12. Z. Komiya, C. Pugh, and R. R. Schrock, *Macromolecules*, **25**, 3609 (1993).
13. M. Brecl and T. Malavasic, *J. Polym. Sci., Part A: Polym. Chem.*, **35**, 2871 (1997).
14. V. D. Athawale, R. S. Bailkeri, and M. Athawale, *Prog. Org. Coat.*, **42**, 132 (2001).
15. J. Nakajima, H. Mochizuki, M. Yamamoto, and H. Wakemoto, *US Patent*, 5087672 (1992).
16. A. A. Craig and C. T. Imrie, *J. Mater. Chem.*, **4**, 1705 (1994).
17. V. Percec and D. Tomazos, *Adv. Mater.*, **4**, 548 (1992).
18. T. Mihara and N. Koide, *Polym. J.*, **29**, 138 (1997).
19. M. Tanaka and T. Nakaya, *Makromol. Chem.*, **190**, 3067 (1989).
20. B. Massoumeh and P. Zhaleh, *React. Funct. Polym.*, **68**, 507 (2008).
21. T. L. Wang, F. J. Huang, and S. W. Lee, *Polym. Int.*, **51**, 1348 (2002).
22. M. Brecl, M. Zigon, and T. Malavasic, *J. Polym. Sci., Part A: Polym. Pol. Chem.*, **36**, 2135 (1998).
23. D. L. Pavia, G. M. Lampman, and G. S. Kriz, "Introduction to Spectroscopy: A Guide for Students of Organic Chemistry", 1st Ed., pp.157-158, W. B. Saunders Company, PA, USA, 1979.
24. J. Gao, Y. Wang, G. Hou, and G. Liu, *J. Appl. Polym. Sci.*, **108**, 1223 (2008).

25. R. N. Jana and J. W. Cho, *J. Appl. Polym. Sci.*, **108**, 2857 (2008).
26. T. M. Wu and E. Chen, *J. Polym. Sci., Part A: Polym. Phys.*, **44**, 598 (2006).
27. A. Abe, Y. Tsuchiya, N. Sugiura, H. Saisho, K. Nishimura, and K. Takeo, *Tissue Cell*, **29**, 191 (1997).
28. M. Krumova, D. Lopez, R. Benavente, C. Mijangos, and J. M. Perena, *Polymer*, **41**, 9265 (2000).
29. J. Xu, J. Bao, B. H. Guo, H. Ma, T. L. Yun, L. Gao, G. Q. Chen, and T. Iwata, *Polymer*, **48**, 348 (2007).
30. Y. Wang, B. Zhang, X. He, and J. W. Wang, *Colloid Polym. Sci.*, **285**, 1077 (2007).
31. S. Kurihara, A. Sakamoto, and T. Nonaka, *Macromolecules*, **32**, 3150 (1999).